

# EXPERIMENTAL INVESTIGATIONS ON VORTEX-INDUCED VIBRATIONS WITH A LONG FLEXIBLE CYLINDER. PART I: MODAL-AMPLITUDE ANALYSIS WITH A VERTICAL CONFIGURATION

Guilherme R. Franzini\*

Celso P. Pesce

Rodolfo T. Gonçalves

Offshore Mechanics Laboratory (LMO), Escola Politécnica (EPUSP), University of São Paulo, Brazil.

André L. C. Fajarra<sup>†</sup>

Pedro Mendes

Department of Mobility Engineering  
Federal University of Santa Catarina, Brazil.

Petrobras Research Center  
(CENPES/PDEP/TDUT), Brazil.

## ABSTRACT

An experimental investigation of Vortex-Induced Vibration (VIV) on a long and vertical flexible cylinder is presented and some results are analyzed. Optical instrumentation allows to directly measure the cartesian coordinates of 43 targets placed along the model. At each instant, modal decomposition based on Galerkin's scheme is applied and, then, modal-amplitude time-histories are obtained. The modal-amplitude time-histories are analyzed, allowing to identify similarities in the modal response at the first and the second natural modes lock-in. Jumps and phase-shifts transitions are also obtained from the analysis of the modal-amplitude time-histories. Finally, it is also found that modal response amplitudes, plotted as functions of the corresponding, reasonable collapses onto the same curve, providing an experimental evidence that the modal response are the same for different excited modes.

*Keywords: Vortex-Induced Vibrations, flexible cylinder, experiments, modal analysis.*

## INTRODUCTION

Vortex-Induced Vibrations (VIV) is a non-linear, self-excited and self-limited fluid-structure interaction phenomenon which may be of crucial importance in structural integrity studies of risers and other slender structures commonly found in the offshore engineering scenario.

A great deal of investigations have been carried out in the last five decades, mostly dedicated to fundamental

aspects of VIV of elastically supported rigid cylinders, as thoroughly described in earlier reviews such as, for example, references [1], [2] and [3]. Flexible cylinders are, however, a much closer representation of risers dynamics. In this context, some aspects such as presence of traveling waves, modal jumps, multimodal excitations, are intrinsic to the dynamics of long flexible cylinders; see, for instance, [4], [5], [6], [7] and [8]. Reference [9] presents a review of flexible cylinders VIV.

Recently, a comprehensive research project on non-linear dynamics of risers was conducted at Escola Politécnica of University of São Paulo. Three groups of experiments with a long and immersed flexible cylinder were carried out for two arrangements - vertical and catenary configurations; namely, (i) pure top-motion (see [10] for results concerning the vertical configuration), (ii) pure VIV, (iii) concomitant VIV and top-motion; details may be found in [11]. Part of the results from the second group of experiments with the vertical configuration are herein presented. Results from the same group, but for a catenary configuration are presented in Part III, [12], of this series of papers, while Part II (see [13]) focuses on results of group (iii) for the vertical configuration.

Instead of a standard VIV analysis (i.e., statistical and spectral analyses for each measurement point along the model), this paper focuses on analyzing the modal-amplitude time-histories obtained after the application of a Galerkin's projection scheme. The objective is to present some aspects enlightened by the modal-amplitude time-histories and examples of analysis that can be carried out with them. It is also discussed on the paper the complimentary character of the modal analysis with re-

\*Corresponding author. Email: gfranzini@usp.br

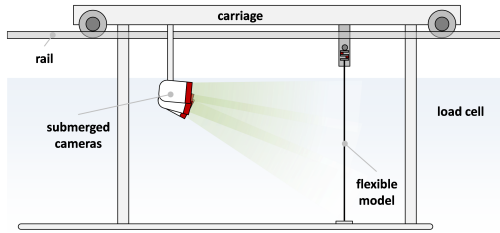
<sup>†</sup>Formerly at University of São Paulo.

spect to the standard analysis.

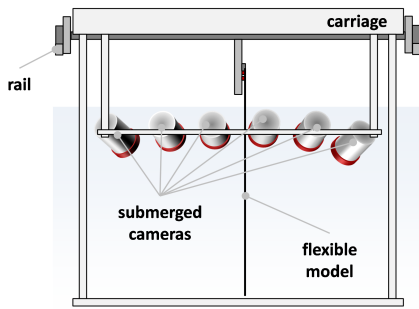
The paper is structured as follows: The next Section presents details regarding the experimental arrangement and the analysis methodology. In the following Section, some results are presented and discussed. Finally, final remarks and perspectives of further works are presented.

## EXPERIMENTAL ARRANGEMENT AND ANALYSIS METHODOLOGY

The experiments were carried out at IPT (Institute for Technological Research of the State of São Paulo) towing tank facility. Reynolds number ranged from 700 to 6100. The cylinder diameter is  $D = 22.2\text{mm}$  with unstretched length  $L_0 = 2552\text{mm}$ . The mass ratio parameter, the immersed to total length and the immersed length to diameter ratios were, respectively, 3.48, 80% and 100. Fig. 1 presents a schematic representation of the experimental arrangement. Main properties<sup>1</sup> of the flexible cylinder are presented in Tab. 1.



(a) Sketch of the side view.



(b) Sketch of the back view.

**FIGURE 1:** Schematic representations of the experimental arrangement. Carriage speed is from left to right.

Displacements of 43 points along the model were measured by an underwater optical tracking system and

<sup>1</sup>Damping ratios refer to experiments carried out in air, with the same corresponding modal stiffness (regulated by tension) as in water [14].

**TABLE 1:** Flexible cylinder properties and characteristics of the vertical configuration.

Cylinder properties			
External diameter $D$	22.2 mm		
Axial stiffness $EA$	1.2 kN		
Bending stiffness $EI$	0.056 Nm <sup>2</sup>		
Linear mass $m_l$	1.19 kg/m		
Immersed weight $\gamma$	7.88 N/m		
Characteristics of the vertical configuration			
Unstretched length $L_0$	2552 mm		
Stretched length $L$	2602 mm		
Immersed length $L_i$	2257 mm		
Mass ratio parameter $m^*$	3.48		
Aspect ratio $L_i/D$	102		
$L/D$	117		
Static tension at the top $T_t$	40 N		
Natural frequencies and modal damping ratios			
mode $n$	$f_{N,n}^{air}$	$\zeta_n$	$f_{N,n}$
1	1.00 Hz	0.42%	0.84 Hz
2	2.05 Hz	0.63%	1.68 Hz
3	3.10 Hz	0.89%	2.52 Hz

the vertical component of the force at the top was measured by a load cell. Data were sampled at  $f_{sp} = 60\text{Hz}$  along 300s of steady-state regime. The flexible cylinder was tensioned by applying a static axial force at the top of 40N. Free-decaying tests carried out with the immersed model at rest indicated that the natural frequency of the  $n$ -mode is given by  $f_{N,n} = n0.84\text{Hz}$  at null towing speed conditions. As presented in [14], the natural frequencies in air roughly follows the relation<sup>2</sup>  $f_{N,n}^{air} = n1\text{Hz}$  and the modal 'structural damping' ratio (w.r.t. the critical value) is lower than 1% for the first three natural modes.

In experimental investigations of flexible cylinders VIV, it is very common the use of strain-gages ([4], [6, 17]) or accelerometers ([18]). These experimental

<sup>2</sup>Actually, eigen modes are Bessel-like functions [15], [16], making the natural frequency ratio deviate from a natural number sequence. This effect is a little more pronounced in air than in water.

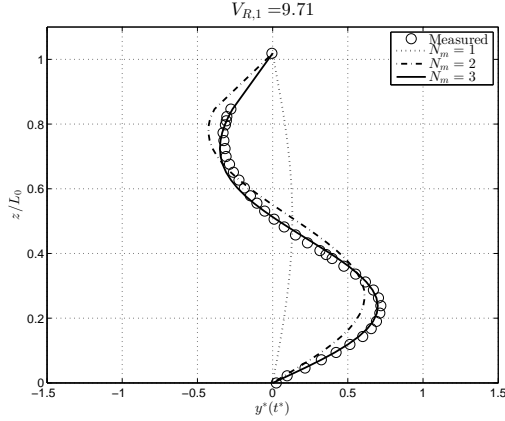


**FIGURE 2:** Example of reconstruction of measured data at a particular instant.

approaches are indirect ways to measure displacements, since they depend either on assumptions regarding the structural modeling or on double integration with respect to time. The large number of points and the direct measurement method allow a richer analysis of the flexible cylinder VIV dynamics.

In fact, from the directly measured displacements, the analysis methodology consists in applying the Galerkin's scheme, i.e., to project the deformed configuration of the flexible cylinder, at an arbitrary instant  $t_j$ , onto the space composed by modal functions  $\psi(z)$ . Being  $X^*(z, t_j)$  and  $Y^*(z, t_j)$  the in-line and cross-wise displacements<sup>3</sup> with respect to the towing direction measured at the point of spanwise coordinate  $z$  at  $t_j$ , the respective modal amplitudes corresponding to a given  $n$ - mode may be written, respectively:

$$\tilde{a}_n^x(t_j) = \frac{\int_0^{L_0} X^*(z, t_j) \psi_n(z) dz}{\int_0^{L_0} (\psi_n(z))^2 dz} \quad (1)$$

$$\tilde{a}_n^y(t_j) = \frac{\int_0^{L_0} Y^*(z, t_j) \psi_n(z) dz}{\int_0^{L_0} (\psi_n(z))^2 dz} \quad (2)$$

Fig. 2 presents an example of reconstruction of the measured cross-wise displacement at a certain instant  $t_j$ . As expected, the increase of the number of modes,  $N_m$ , used in the reconstruction leads to a better representation of the measured data.

Similarly to [6], [17] and [19], the mode functions considered herein are sinusoidal ones  $\psi_n(z) = \sin(n\pi z/L_0)$ . Evidently, much more representative mode functions could be used, as the classic Bessel's, which neglect bending and axial stiffness effects (see, e.g.,

[15]), or Bessel-like ones, which incorporate both effects through an ingenious integral averaging procedure; see [16]. Nonetheless, sinusoidal functions, besides simpler, are here considered as sufficient to exemplify the analysis methodology. Consistently, the modal reduced velocity can be defined by normalizing the free-stream velocity  $U_\infty$  by the product between the diameter and the  $n$ - natural frequency  $f_{N,n}$ . Hence:

$$V_{R,n} = \frac{U_\infty}{f_{N,n} D} \quad (3)$$

Another aspect of potential interest in the study of the flexible cylinder VIV is the synchronization between in-line and cross-wise oscillation. The modal amplitude time-histories allow not only the study of synchronization between natural modes in orthogonal directions but also natural modes in the same direction, such as, for example, synchronization between the first and second modes in the cross-wise direction.

In this paper, synchronization is investigated by considering the time-history of phase-shift between two modal amplitude time-histories. Following the definition presented in [20], synchronization is characterized by a time-invariant phase-shift between two signals. In the VIV context, synchronization analysis was carried out by [19] in for flexible cylinder VIV (not considering modal-amplitude time-histories) and by [21] addressing of phase-shift between force and displacement in 2-dof VIV.

Let  $w(t)$  be a signal and  $\mathbf{H}(w)$  its Hilbert Transform. The Hilbert Transform allows representing the instantaneous phase ( $\phi_w(t)$ ) and amplitude  $a_w(t)$  of  $w(t)$ , in the form:

$$\mathbf{H}(w) = a_w(t) e^{j\phi_w(t)} \quad (4)$$

The phase-shift between two signals is then given by

$${}^m_n \phi_p^q(t) = -\beta \phi_n^p(t) + \phi_m^q(t) \quad (5)$$

where  $n$  and  $m$  refer to the mode number,  $p$  and  $q$  indicate the direction (in-line or cross-wise) and  $\beta$  is the ratio between the dominant frequency of the two signals. Although Eqn. 5 can be used both for modes in orthogonal directions as well as in the same direction, synchronization analyses between modes in the same direction is not herein carried out for the sake of conciseness of this paper. This is left for a further work.

<sup>3</sup>All displacement amplitudes are normalized by the diameter  $D$ .

## RESULTS AND DISCUSSIONS

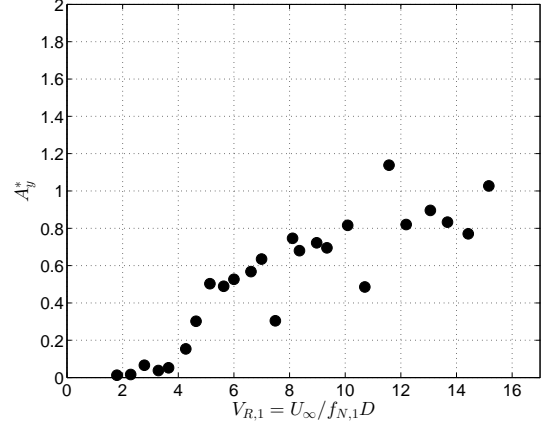
Firstly, it will be discussed how the modal analysis proposed in the previous section may help as a complementary tool for the standard analysis. Fig. 3 shows a standard analysis of the cross-wise displacements measured at  $z/L_0 = 0.22$ . Fig. 3(a) presents the characteristic oscillation amplitude (obtained by averaging the 10% of the highest peaks). For reduced velocities  $V_{R,1} = U_\infty/f_{N,1}D < 8$ , there is a qualitative agreement with the results obtained with a rigid cylinder elastically supported. However, due to the onset of the second natural mode lock-in, a classical lower branch for  $V_{R,1} > 8$  is not observed. The non-dimensional amplitude spectra presented in 3(b) reveals the presence of lock-in with distinct natural modes depending on the value of  $V_{R,1}$ . Although interesting, both graphics are not sufficient to discuss the contribution of the distinct natural modes in the flexible cylinder VIV. The modal decomposition appears as a useful scheme for the mentioned analysis and examples of use will be addressed below.

The first example of use of the modal analysis technique refers to the case in which the lock-in is observed in the first natural mode; in the present experiments at  $V_{R,1} = U_\infty/f_{N,1}D = 5.63$ . Fig. 4(a) presents the modal amplitude time-history corresponding to the first vibration mode, i.e.,  $n = 1$  in Eqns. 1 and 2.

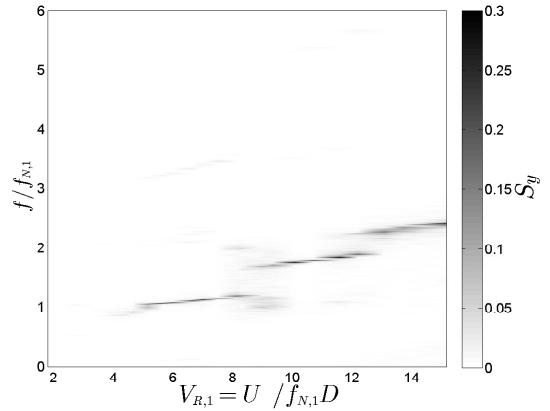
As expected the modal-amplitude time-history  $\tilde{a}_1^y(t)$  is practically monochromatic at the first natural frequency. It is well known from the literature addressing rigid cylinders mounted on two degrees-of-freedom elastic supports (see, for example, [22]) that the in-line vibration takes place at twice the cross-wise vibration frequency. Hence, it seems natural that, for the first mode lock-in, the second natural mode might be excited in the in-line direction. This fact is confirmed in Fig. 4(b), showing a well defined “eight-shaped” figure in the  $\tilde{a}_1^y(t) \times \tilde{a}_2^x(t)$  modal amplitude plane; a neat experimental example of dual resonance (see [23]).

Still considering the first-mode lock-in, it is interesting to investigate the synchronization between  $\tilde{a}_1^y(t^*)$  and  $\tilde{a}_2^x(t^*)$ . Fig. 5 presents the temporal evolution of the phase-shift  ${}^2_1\phi_y^x$  and the corresponding histogram normalized by the total number of occurrences. Notice that  ${}^2_1\phi_y^x$  is practically time-invariant and close to  $50^\circ$ . Hence, the first mode lock-in is accompanied by a very well-defined synchronization between first natural mode oscillations in the cross-wise direction and second natural mode oscillations in the in-line direction.

Consider now the second mode lock-in and, for this, a test condition in which the modal reduced velocity cor-



(a) Characteristic cross-wise oscillation amplitude at  $Z/L_0 = 0.22$ .



(b) Non-dimensional cross-wise amplitude spectra.

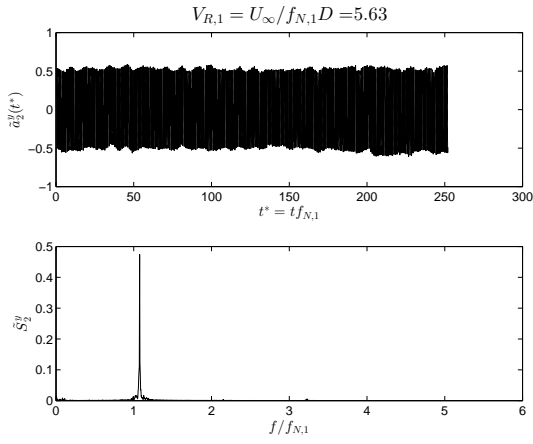
**FIGURE 3:** Results for cross-wise displacements at  $z/L_0 = 0.22$

responding to the second natural mode is  $V_{R,2} = 5.78^4$ . Fig. 6 presents both the cross-wise modal amplitude time-history and the projection in the plane  $\tilde{a}_2^y \times \tilde{a}_4^x$ .

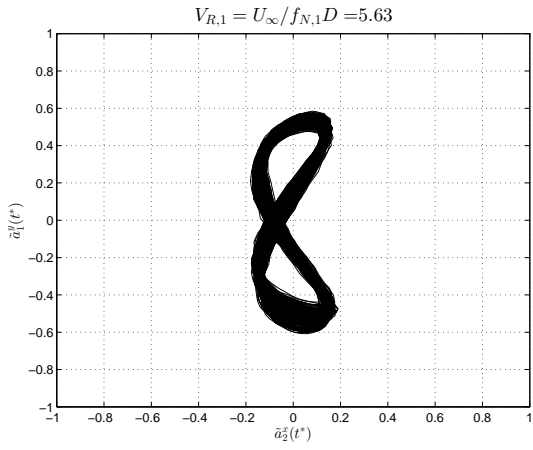
Fig. 6(a) clearly reveals two regimes. In the first one ( $t^* = t f_{N,1} < 15$ ), the characteristic amplitude is similar to that observed in  $\tilde{a}_1^y(t)$  when  $V_{R,1} = 5.68$  (see Fig. 4(a)), i.e., at practically the same modal reduced velocity. The second regime is characterized by an increase in the characteristic amplitude. The trajectories in the  $\tilde{a}_2^y(t) \times \tilde{a}_4^x(t)$  plane, presented in Fig. 6(b), reveal that the increase of amplitude in  $\tilde{a}_2^y(t)$  is accompanied by a decrease in  $\tilde{a}_4^x(t)$ . In the first regime, a classic eight-shaped trajectory in the  $\tilde{a}_2^y(t) \times \tilde{a}_4^x(t)$  is also shown in red, similar to what appeared in the first mode lock-in. Nonetheless, such regime quickly jumps to another one, where relative phases change and a C-shaped trajectory prevails. This

<sup>4</sup>Notice that the value of this modal reduced velocity is very similar to that previously investigate.

is for sure an interesting phenomenon, possibly revealing the co-existence of two dynamic attractors.



(a) Modal-amplitude time-history  $\tilde{a}_1^y(t)$ .



(b) Trajectory in the  $\tilde{a}_1^y(t) \times \tilde{a}_2^x(t)$  plane.

**FIGURE 4:** Modal-amplitude time-histories.  $V_{R,1} = 5.63$ .

It remains of interest the discussion regarding the synchronization between modal amplitude time-histories in cross-wise and in-line directions. For this, consider Fig. 7. In this plot, it is clearly noticeable a sudden phase jump from  $\frac{4}{2}\phi_y^x \approx 230^\circ$  to  $\frac{4}{2}\phi_y^x \approx 45^\circ$  at  $t^* \approx 15$ . Furthermore, considering  $t^* > 15$ , the phase-shift time-history is much more oscillatory, compared to the case corresponding to  $V_{R,1} = 5.63$ , presented in Fig. 5. Hence, despite the first and second natural modes lock-in indicate similar qualitative behavior of the phase-shifts, the phase modulation is more pronounced on the latter case, indicating a less defined synchronization.

The last result herein presented consists in plotting the characteristic values,  $\tilde{A}_n^x$  and  $\tilde{A}_n^y$ , as functions of the modal reduced velocity  $V_{R,n} = U_\infty / f_{N,n}D$ . The characteristic values were computed by averaging the 10% of the

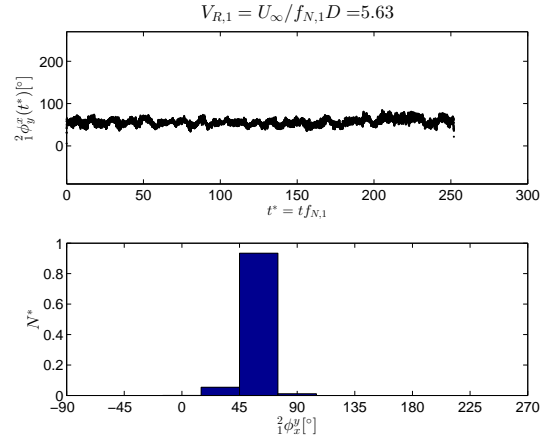
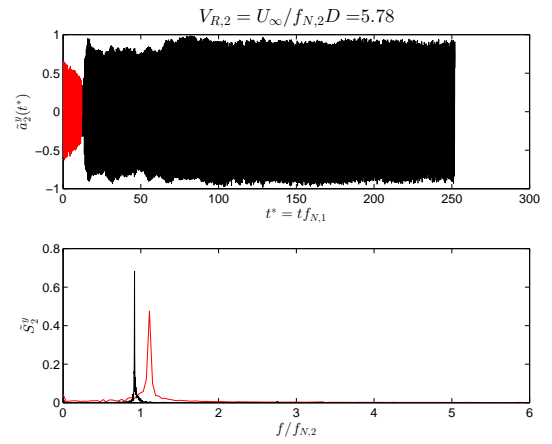
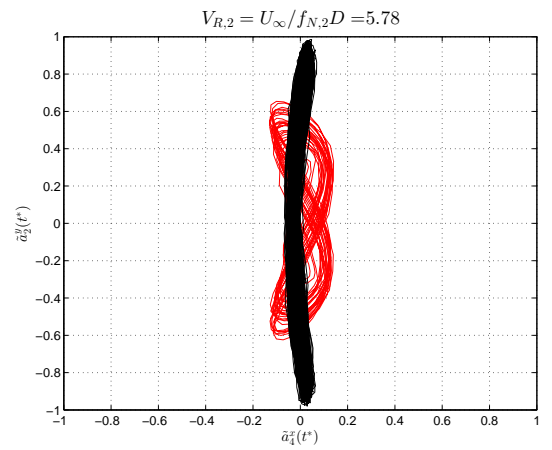


**FIGURE 5:** Phase-shift between  $\tilde{a}_1^y(t^*)$  and  $\tilde{a}_2^x(t^*)$ .  $V_{R,1} = 5.63$ .



(a) Modal-amplitude time-history  $\tilde{a}_2^y(t)$ .



(b) Trajectory in the  $\tilde{a}_2^y(t) \times \tilde{a}_4^x(t)$  plane.

**FIGURE 6:** Modal-amplitude time-histories.  $V_{R,2} = 5.78$ .

highest modal-amplitude time-histories peaks. As can be seen in Fig. 8, the values of amplitude  $\tilde{A}_i^y$  follow the same trend for the first four natural modes. Furthermore, the re-

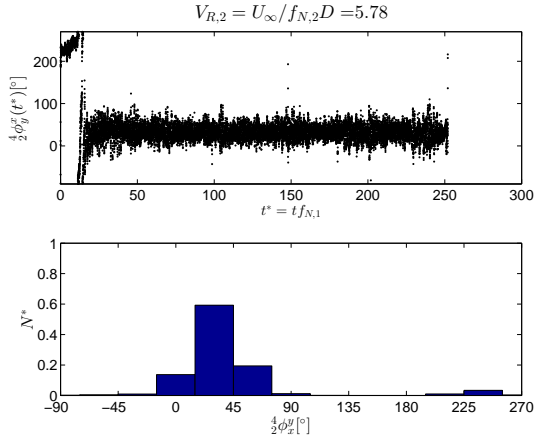
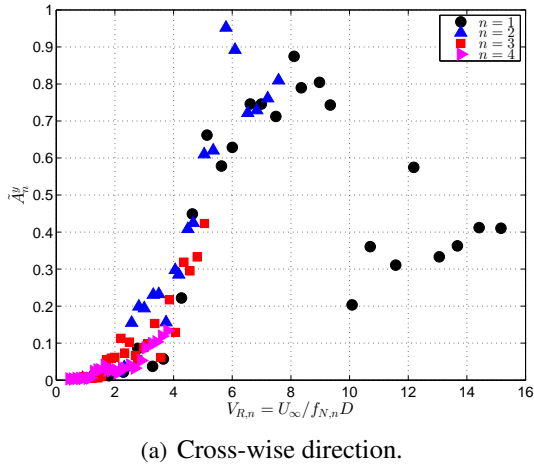
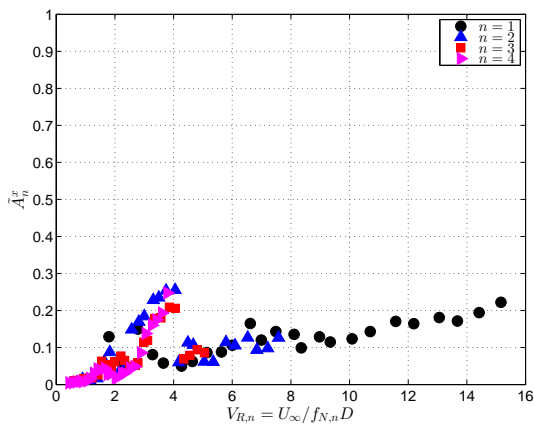


**FIGURE 7:** Phase-shift between  $\tilde{a}_2^y(t^*)$  and  $\tilde{a}_4^x(t^*)$ .  $V_{R,2} = 5.78$ .

response is remarkably similar to those usually encountered for elastically supported rigid cylinders.



(a) Cross-wise direction.



(b) In-line direction.

**FIGURE 8:** Characteristic values of modal-amplitudes as a function of modal reduced velocity.

## FINAL REMARKS

The present paper presented experimental results of a long, vertical and flexible cylinder subjected to Vortex-Induced Vibrations (VIV). The cartesian coordinates of 43 reflexive targets placed along the model were directly measured by an optical tracking system. Such optical measuring technique, along with a Galerkin's decomposition scheme, formed an innovative experimental analysis procedure, leading to a direct evaluation of modal-amplitude time-histories in both, in-line and cross-wise directions.

Some interesting aspects were enlightened through the analysis of the modal-amplitude time-histories. The first-mode lock-in is characterized by a steady-state response with a remarkable synchronization between the modal-amplitude time-histories associated to the first mode in cross-wise direction and the second mode in in-line direction. On the other hand, considering the second-mode lock-in, two regimes in the response were clearly identified. The first regime has a remarkable similarity with the one observed for the first-mode lock-in. The second one is characterized by an increase in the cross-wise oscillations and a decrease in the in-line amplitudes. These two distinct regime also present slightly different spectral distributions.

The characteristic values of the modal-amplitude time-histories were also evaluated. Plotting these results as functions of the modal reduced velocity (i.e, the reduced velocity considering the natural frequency of each mode), the same trend for all the modes was obtained.

Ongoing researches include a deeper analysis of the modal-amplitude time-histories, such as the use of time-frequency domain signal analysis techniques in order to better identify mode transitions and jumps in the response. Further analysis of synchronization between modes in orthogonal directions and synchronization between modes in the same direction are being carried out.

Part I took care of the vertical configuration subjected to pure VIV, pertaining to experimental group (ii). In this same conference, Part II, addresses experimental group (iii), studying the effect of axial motion excitation in the VIV of the same vertical configuration; whereas Part III takes care of pure VIV in a catenary configuration, pertaining to group (ii).

## ACKNOWLEDGMENT

The results presented in the paper were obtained from a comprehensive research project on non-linear dynamics of risers sponsored by Petrobras and carried out in 2011-2013. First and third authors ac-

knowledge FAPESP (São Paulo Research Foundation) for their post-doctoral scholarship, grants 2013/09802-2 and 2014/02043-1. The National Council for Research, CNPq, is acknowledged by first, second and fourth authors for the grants 3310595/2015-0, 308990/2014-5 and 309591/2013-9. Special thanks to the IPT towing tank technical staff.

## REFERENCES

- [1] Bearman, P. W., 1984. "Vortex shedding from oscillating bluff bodies". *Annual Review of Fluid Mechanics*, **16**, Jan, pp. 195–222.
- [2] Williamson, C. H. K., and Govardhan, R. N., 2004. "Vortex-induced vibrations". *Annual Review of Fluids Mechanics*, **36**, pp. 413–455.
- [3] Sarpkaya, T., 2004. "A critical review of the intrinsic nature of vortex-induced vibrations". *Journal of Fluids and Structures*, **19**, pp. 389–447.
- [4] Pesce, C. P., and Fujarra, A. L. C., 2000. "Vortex-induced vibrations and jump phenomenon: Experiments with a clamped flexible cylinder in water". *International Journal of Offshore and Polar Engineering*, **10**, pp. 26–33.
- [5] Facchinetti, M. L., de Langre, E., and Biolley, F., 2004. "Vortex-induced traveling waves along a cable". *European Journal of Mechanics B/Fluids*, **23**, pp. 199–208.
- [6] Chaplin, J. R., Bearman, P. W., Huera Huarte, F. J., and Pattenden, R. J., 2005. "Laboratory measurements of Vortex-Induced Vibrations of a vertical tension riser in a stepped current". *Journal of Fluids and Structures*, **21**, pp. 3–24.
- [7] Swithenbank, S., 2007. "Dynamics of long flexible cylinders at high-mode number in uniform and sheared flows". PhD thesis, Massachusetts Institute of Technology.
- [8] Vandiver, J. K., Jaiswal, V., and Jhingran, V., 2009. "Insights on vortex-induced, traveling waves on long risers.". *Journal of Fluids and Structures*, **25**, pp. 641–653.
- [9] Wu, X., Ge, F., and Hong, Y., 2012. "A review of recent studies on vortex-induced vibrations of long slender cylinders". *Journal of Fluids and Structures*, **28**, pp. 292–308.
- [10] Franzini, G. R., Pesce, C. P., Salles, R., Gonçalves, R. T., Fujarra, A. L. C., and Mendes, P., 2015. "Experimental investigation with a vertical and flexible cylinder in water: response to top motion excitation and parametric resonance". *Journal of Vibration and Acoustics*, **137** (3), pp. 031010–1 – 031010–12.
- [11] Pesce, C. P., 2013. Riser dynamics: experiments with small scale models. LabOceano - Ten-Years Anniversary Celebration Workshop, April 29-30.
- [12] Rateiro, F., Fujarra, A. L. C., Pesce, C. P., Gonçalves, R. T., Franzini, G. R., and Mendes, P., 2016. "Experimental investigations on vortex-induced vibrations with a long flexible cylinder. Part III: modal-amplitude analysis with a catenary configuration". In Proceedings of the 11th International Conference on Flow-Induced Vibration.
- [13] Franzini, G. R., Pesce, C. P., Gonçalves, R. T., and Mendes, P., 2016. "Experimental investigations on Vortex-Induced Vibrations with a long flexible cylinder. Part II: effect of axial motion excitation in a vertical configuration.". In Proceedings of the 11th International Conference on Flow-Induced Vibration.
- [14] Salles, R., 2016. "Experimental analysis of fluid-structure interaction phenomena on a vertical flexible cylinder: modal coefficients and parametric resonance". Master's thesis, Escola Politécnica da Universidade de São Paulo.
- [15] Pesce, C. P., Fujarra, A. L. C., Simos, A. N., and Tannuri, E. A., 1999. "Analytical and closed form solutions for deep water riser-like eigenvalue problem". In Proceedings of the Ninth (9th) International Offshore and Polar Engineering Conference.
- [16] Mazzilli, C. E. N., Lenci, S., and Demeio, L., 2014. "Non-linear free vibrations of tensioned vertical risers". In Proceedings of the 8th European Nonlinear Dynamics Conference - ENOC2014.
- [17] Chaplin, J. R., Bearman, P. W., Cheng, Y., Fontaine, E., Graham, J. M. R., Herfjord, K., Huera Huarte, F. J., Isherwood, M., Lambracos, K., Larsen, C. M., Meneghini, J. R., Moe, G., Pattenden, R., Triantafyllou, M. S., and Willden, R. H. J., 2005. "Blind predictions of laboratory measurements of Vortex-Induced Vibrations of a tension riser". *Journal of Fluids and Structures*, **21**, pp. 25–40.
- [18] Huang, S., Khorasanchi, M., and Herfjord, K., 2011. "Drag amplification of long flexible riser models undergoing multi-mode VIV in uniform currents". *Journal of Fluids and Structures*, **27**, pp. 342–353.
- [19] Huera-Huarte, F. J., and Bearman, P. W., 2009. "Wake structures and vortex-induced vibrations of a long flexible cylinder - part 1: dynamic response". *Journal of Fluids and Structures*, **25**, pp. 969–990.
- [20] Pikovsky, A., Rosenblum, M., and Kurths, J., 2001. *Synchronization - A Universal Concept in Nonlinear Sciences*. Cambridge University Press.
- [21] Franzini, G. R., Gonçalves, R. T., Meneghini, J. R.,

and Fujarra, A. L. C., 2013. “One and two degrees-of-freedom vortex-induced vibration experiments with yawed cylinders”. *Journal of Fluids and Structures*, **42**, pp. 401–420.

- [22] Jauvtis, N., and Williamson, C. H. K., 2004. “The effect of two degrees of freedom on vortex-induced vibration at low mass and damping”. *Journal of Fluid Mechanics*, **509**, pp. 23–62.
- [23] Dahl, J. M., Hover, F. S., Triantafyllou, M. S., and Oakley, O. H., 2010. “Dual resonance in vortex-induced vibrations at subcritical and supercritical Reynolds numbers”. *Journal of Fluid Mechanics*, **643**, pp. 395–424.